View metadata, citation and similar papers at core.ac.uk

brought to you by CORE

Bioresource Technology 208 (2016) 64–72

Contents lists available at ScienceDirect

Bioresource Technology

journal homepage: www.elsevier.com/locate/biortech

# Cathodic bacterial community structure applying the different co-substrates for reductive decolorization of Alizarin Yellow R

Qian Sun [a], Zhi-Ling Li [a], You-Zhao Wang [b], Chun-Xue Yang [a], Jong Shik Chung [c,d], Ai-Jie Wang [a,e,*]

[a] State Key Laboratory of Urban Water Resource and Environment, Harbin Institute of Technology (SKLUWRE, HIT), No. 73 Huanghe Road, Harbin 150090, PR China
[b] School of Mechanical Engineering and Automation, Northeastern University, Shenyang 110004, PR China
[c] Department of Chemical Engineering, Pohang University of Science and Technology (POSTECH), San 31, Hyoja-dong, Pohang 790-784, South Korea
[d] Division of Environmental Catalysis, Research Institute of Industrial Science and Technology, P.O. Box 135, Pohang 790-600, South Korea
[e] Research Center for Eco-Environmental Sciences, Chinese Academy of Sciences, Beijing, 100085, PR China

## HIGHLIGHTS

- Feeding with glucose obtained higher AYR decolorization efficiency than acetate.
- Diverse cathodic bacterial communities were observed with different co-substrates.
- Glucose-fed condition was dominated with *Citrobacter*, *Enterococcus* and *Alkaliflexus*.
- Acetate-fed condition was dominated with Acinetobacter and Achromobacter.
- Co-substrate types impacted performance and the cathodic bacterial communities.

## ARTICLE INFO

*Article history:*
Received 27 November 2015
Received in revised form 31 January 2016
Accepted 1 February 2016
Available online 6 February 2016

*Keywords:*
Biocathode
Bioelectrochemcial system (BES)
Reductive decolorization
Alizarin Yellow R (AYR)
Bacterial community structure

## ABSTRACT

Selective enrichment of cathodic bacterial community was investigated during reductive decolorization of AYR fedding with glucose or acetate as co-substrates in biocathode. A clear distinction of phylotype structures were observed between glucose-fed and acetate-fed biocathodes. In glucose-fed biocathode, *Citrobacter* (29.2%), *Enterococcus* (14.7%) and *Alkaliflexus* (9.2%) were predominant, and while, in acetate-fed biocathode, *Acinetobacter* (17.8%) and *Achromobacter* (6.4%) were dominant. Some electroactive or reductive decolorization genera, like *Pseudomonas*, *Delftia* and *Dechloromonas* were commonly enriched. Both of the higher AYR decolorization rate ($k_{AYR}$ = 0.46) and *p*-phenylenediamine (PPD) generation rate ($k_{PPD}$ = 0.38) were obtained fed with glucose than acetate ($k_{AYR}$ = 0.18; $k_{PPD}$ = 0.16). The electrochemical behavior analysis represented a total resistance in glucose-fed condition was about 73.2% lower than acetate-fed condition. The different co-substrate types, resulted in alteration of structure, richness and composition of bacterial communities, which significantly impacted the performances and electrochemical behaviors during reductive decolorization of azo dyes in biocathode.

© 2016 Elsevier Ltd. All rights reserved.

## 1. Introduction

Millions of tons of dye-laden wastewater are generated from textile industries in the world each year. The appropriate treatment strategy of these wastes before discharge is desirable for both market and environment demand. The dyes cover various structural features, such as the ones contain azo/diazo bond, anthraquinone-based, metal-complex, etc. Among them, azo dye with properties of toxic, mutagenic and persistent, presents the largest class applied in textile processing industries (van der Zee and Villaverde, 2005).

Decolorization of azo dyes by anaerobic microorganisms through azo bond cleavage has been regarded as a cost-efficient approach. So far, various types of bacteria have been reported that possess azo dye decolorization capacities, including genera of *Pseudomonas*, *Acinetobacter*, *Citrobacter*, *Comamonas* and *Pannonibacter* (Hsueh and Chen, 2008; Iyappan et al., 2010; Stolze et al., 2012; Wang et al., 2009a,b). After decolorization, azo dye was decomposed to less toxic and easily degradable aromatic amines, such as *p*-phenylenediamine (PPD) and 5-aminosalicylic acid (5-ASA) during reduction of Alizarin Yellow R (AYR) (Cui et al., 2014). However, the anaerobic process involves the long decomposition period

* Corresponding author at: State Key Laboratory of Urban Water Resource and Environment, Harbin Institute of Technology (SKLUWRE, HIT), No. 73 Huanghe Road, Harbin 150090, PR China. Tel./fax: +86 451 86282195.
*E-mail address:* waj0578@hit.edu.cn (A.-J. Wang).

http://dx.doi.org/10.1016/j.biortech.2016.02.003
0960-8524/© 2016 Elsevier Ltd. All rights reserved.

based on the low metabolic rate of bacteria and to some extent restricts the application perspective.

In recent years, bioelectrochemical systems (BESs) have been extensively explored for the enhanced reduction of recalcitrant organic pollutants in biocathode, such as chloramphenicols, nitrobenzenes, azo dyes and etc.(Huang et al., 2011), also should be pay more attention on the hidden potential food and agriculture wastewater used as substrates in MFC for power generation with simultaneous treatment wastewater (ElMekawy et al., 2015). The enhanced reductive decolorization of azo dyes by inoculating the reductive consortia has been widely investigated focusing on decolorization kinetic behavior, such as the removal effect and efficiency and intermediate or end metabolites in some configuration modified BESs (Cui et al., 2012). In these systems, organic substrates were usually amended as co-substrates, such as acetate, propionate, lactate, glucose, and cellulose, etc. (Sun et al., 2009).

In the practical azo dye contaminated wastewater, water quality is varied from the nutrient-rich heterotrophic environment to the oligotrophic environment, thus it is meaningful for estimating azo dye removal efficiency with the functional biocathode communities upon the different organic substrates supply. So far, few report has shown how practical and switched substrates, affect the cathodic bacterial community structures, especially for azo dye decolorization process. Some studies investigated the cathodic biofilm communities for azo dye reduction using traditional PCR-DGGE and clone libraries by comparison of the decolorization activities with or without addition of congo red (Sun et al., 2013) but these studies were lack of sufficient sequences to capture the comprehensive and systematic information on the diverse bacterial communities. In addition, the clear alteration of bacterial composition from the initial decolorizing inoculum to the decolorizing cathodic biofilms in response to the different organic substrates is poorly understood. The MiSeq sequencing, focused on 16S rRNA gene with a high taxonomic resolution, is considered suitable for characterizing bacterial community structure in reduction of biocathode biofilm (Liang et al., 2014).

In this study, both the azo dye decolorization efficiencies and the microbial phylogenetic communities in the initial inoculum and the azo dye decolorizing biocathode biofilms supplying the different substrates (glucose or acetate) were investigated in the acclimated biocathode. Objectives of this study were to (i) determine the impact of organic substrates on the catalytic effects and performance of azo dye decolorization and (ii) characterize the alteration of bacterial phylogenetic communities in the initial inoculum and the azo dye decolorizing biocathode biofilms by supplying the different co-substrates.

## 2. Methods

### 2.1. BES construction, operation, medium composition and inoculum

The dual-chamber BESs were separated by a cationic exchange membrane (5 cm diameter) (CEM, Ultrex CMI-700, Membrane International, U.S.) with the working volume of each chamber of 80 mL. Carbon brushes with diameter of 4.5 cm and length of 4 cm (TOHOTENAX Co. Ltd., China) were applied as anode and cathode. A saturated calomel electrode (SCE, +247 mV vs. Standard hydrogen electrode, SHE, Shanghai Precision Scientific Instruments Co. Ltd, China) was placed in cathode chamber to measure the electrode potentials. Reactors were running in the closed circuit mode using a DC power (IT6921, Itech Co. Ltd., USA) under the external resistance of 20 Ω (Cui et al., 2014). The data of electrode potential and current were collected every ten minutes using a data acquisition (Keithley 2700, Keithley Co. Let., U.S.). All constructed BESs were sealed with sealant to maintain the anaerobic environment. All tests were performed at a constant room temperature of 25 °C.

Alizarin Yellow R (AYR) was selected as the aim pollutant in this study (Tan et al., 1999). The compositions of artificial wastewater supplied in cathode and anode chamber were as follows (g $L^{-1}$): $Na_2HPO_4{\cdot}12H_2O$: 11.55; $NaH_2PO_4{\cdot}2H_2O$: 2.77; $NH_4Cl$: 0.31; KCl: 0.13. Other than this, cathode was additionally applied with glucose (1 g $L^{-1}$) or sodium acetate (1 g $L^{-1}$) as carbon source and possible electrons donors, and while AYR was applied as the objective pollutant in cathode chamber. All reactors were inoculated with 10 mL of activated sludge (total suspended solids of 15,695 ± 260 g $L^{-1}$; soluble carbohydrate of 35 ± 5 mg COD $L^{-1}$) collected from Taiping wastewater treatment plant (Harbin, China). All reactors were simultaneously constructed with two parallel reactors holding the same condition. The applied AYR concentration and the external voltage were set at 100 mg $L^{-1}$ and 0.5 V, respectively.

### 2.2. Chemical, electrochemical and statistical analysis

Liquids were sampled and immediately filtered through a 0.45 μm membrane. AYR was measured using a UV-visible spectrophotometer (UV-1800 spectrophotometer, MAPADA Incorporation, Shanghai, China) at a wavelength of 374 nm. The decolorization products of AYR, *p*-phenylenediamine (PPD), were measured using HPLC (Waters mode e2695, Waters Incorporation, USA) equipped with a Water Symmetry C18 column (5 μm; 4.6 × 250 mm, Waters Incorporation, USA) at 35 °C and a UV/visible detector (model-2489, Waters Incorporation, USA) at 288 and 368 nm, respectively (Sun et al., 2015). The applied mobile phase was methanol:$H_2O$:acetic acid (8:2:0.03) at a flow rate of 1.0 mL $min^{-1}$.

Cyclic voltammetry (CV) was applied to illustrate the catalytic behavior for AYR reduction in system using electrochemical workstation (model-660D, CH Instruments Inc., U.S.) with glassy carbon electrode as the working electrode and the saturated calomel reference electrode (SCE) as the reference electrode. The scan potential ranged from 0 to −1.2 V with the scan rate of 1 mV $s^{-1}$ (Sun et al., 2015). Electrochemical impedance spectroscopy (EIS) measurements were carried on open circuit condition at a frequency range of 0.01–105 Hz with a perturbation signal of 10 mV. The Nyquist plots obtained from EIS experiments were fitted with ZSIMPWIN software to obtain the polarization resistances. The equivalence circuit of *R* was used to simulate EIS results, based on the resistance of duel chamber BES which was consisted of ohmic resistance ($R_{ohm}$), charge transfer resistance ($R_{ct}$) and diffusion resistance ($R_{diff}$) (Sun et al., 2015).

AYR decolorization efficiency (DE) was calculated by the removed AYR concentration divided by the initial AYR concentration, as shown in the following equations:

$$DE = \frac{C_{\text{in-AYR}} - C_{\text{eff-AYR}}}{C_{\text{in-AYR}}} \times 100 \quad (1)$$

where $C_{\text{in-AYR}}$ is the initial AYR concentration, g $L^{-1}$; $C_{\text{eff-AYR}}$ is the time-point AYR concentration, g $L^{-1}$; The rates of AYR reduction and PPD formation were fitted using an apparent first-order reaction model: $C = C_0 e^{-k_{AYR}t}$ and $C = C_0(1 - e^{-k_{PPD}t})$, respectively, where *C* represent AYR or PPD concentration (mg $L^{-1}$) at time *t* (h). $C_0$ is the initial AYR concentration or maximum PPD production concentration. The rate constant *k* ($h^{-1}$) was calculated using Sigma Plot V12.5.

### 2.3. High-throughput 16S rRNA gene MiSeq sequencing and phylogenetic classification

After the continuous running for two weeks (about 15 HRT cycles) under the applied voltage of 0.5 V, the external resistance

of 20 ohm and the initial AYR concentration of 100 mg/L, the data of potential, current and decolorization rate were tended to be stable and the system was considered as the steady state. The cathode biofilms were randomly harvested with a sterilized scissor and stored in 5 mL sterile plastic test tubes with the volume of about 3 mL at −80 °C. DNA was extracted using the OMEGA Soil DNA Isolation kit (OMEGA Bio-Tek Inc, USA) according to the manufacturer's instructions. Concentration and purity of the extracted DNA were measured with Qubit 2.0 photometer (Life Technologies, Inc, USA). Amplicon libraries were constructed for Illumina MiSeq sequencing using bacterial primers 341F (5′ CCTACACGACGCTCTTCCGATCTN (barcode) CCTACGGGNGG CWGCAG 3′) and 805R (5′ GACTGGAGTTCCTTGGCACCCGAGAATTCCAGACTAC HVGG GTATCTAATCC 3′) for the V3–V4 region of the 16S rRNA gene. The fused forward primer includes a 10-nucleotide barcode inserted the primer 341F. The barcodes were used to sort multiple samples in a single MiSeq run. After being purified and quantified, a mixture of amplicons was used for sequencing on an Illumina MiSeq according to standard protocols. To minimize the effects of random sequencing errors, low-quality sequences were removed by elimination those that without an exact match to the forward primer, without a recognizable reverse primer, length shorter than 200 nucleotides and contained any ambiguous base calls (Ns). The barcodes and primers were trimmed from the resulting sequences. Finally, sequencing produced 4078 (glucose-fed biocathode), 4359 (acetate-fed biocathode), and 11,580 (RAW) high-quality V3–V4 tags of the 16S rRNA gene with an average length of 420 bp. Sequences were clustered into operational taxonomic units (OTUs) by setting a 0.03 distance limit (equivalent to 97%). After phylogenetic allocation of the sequences down to the phylum, class and genus level, relative abundance of them calculated. Hierarchical cluster analysis of three tested samples was performed using Cluster v3.0 and visualized by TREEVIEW (http://rana.stanford.edu/). Illumina MiSeq sequencing data was deposited in the NCBI Sequence Read Archive under Bioproject Number SRP065473.

## 3. Results and discussion

### 3.1. AYR reductive decolorization in glucose/acetate-fed biocathode

After two weeks operation, the anode potential below about −450 mV and the cathode potential below −950 mV was the steady state. At this state, reductive decolorization of AYR and the corresponding generated metabolites fed with glucose/acetate as co-substrates were shown in Fig. 1. Within 24 h, AYR could be completely removed under all of the conditions, however, the one fed with glucose showed the higher removal efficiency than that fed with acetate in both closed and open circuits (Fig. 1A). The highest removal efficiency was achieved in glucose-fed close-circuit BES, that within 4 h, AYR removal efficiency approached to 85%. AYR removal rate fitted well with the first-order kinetics. The dynamic response constant $k_{AYR}$ was arranged as follows: glucose-fed closed biocathode ($k_{AYR} = 0.46 \pm 0.06\ h^{-1}$, $r^2 = 0.97$) > acetate-fed closed biocathode ($k_{AYR} = 0.18 \pm 0.01\ h^{-1}$, $r^2 = 0.99$) > glucose-fed open biocathode ($k_{AYR} = 0.16 \pm 0.06\ h^{-1}$, $r^2 = 0.98$) > acetate-fed open biocathode ($k_{AYR} = 0.12 \pm 0.02\ h^{-1}$, $r^2 = 0.95$) (Supplementary information SI Table S1). The $k_{AYR(glucose)}/k_{AYR(acetate)}$ was 1.25 and 2.56 under open- and closed-circuit conditions, respectively.

Two main products, PPD and 5-aminosalicylic acid (5-ASA), were generated during AYR reductive decolorization (Sun et al., 2015). However, 5-ASA is rather instable and tended to be further degraded by anaerobic bacteria, and in comparison, the recovery rate of PPD can be achieved at 100% (Sun et al., 2015). So PPD was selected as the representative of AYR decolorization metabolite in this study. After 24 h, the generated PPD was about 35 mg $L^{-1}$ (about 0.32 mM) and the highest recovery rate of PPD was approached at 94.1% (the initial AYR of 0.34 mM), indicating the complete reductive decolorization of AYR (Fig. 1B). Rates of PPD generation fitted well with the first-order kinetics, with the dynamic response constant $k_{AYR}$ arranged as follows: glucose-fed closed biocathode ($k_{PPD} = 0.38 \pm 0.04\ h^{-1}$, $r^2 = 0.99$) > acetate-fed closed biocathode ($k_{PPD} = 0.16 \pm 0.02\ h^{-1}$, $r^2 = 0.99$) > glucose-fed open biocathode ($k_{PPD} = 0.12 \pm 0.04\ h^{-1}$, $r^2 = 0.95$) > acetate-fed open biocathode ($k_{PPD} = 0.04 \pm 0.02\ h^{-1}$, $r^2 = 0.99$) (SI Table S1).

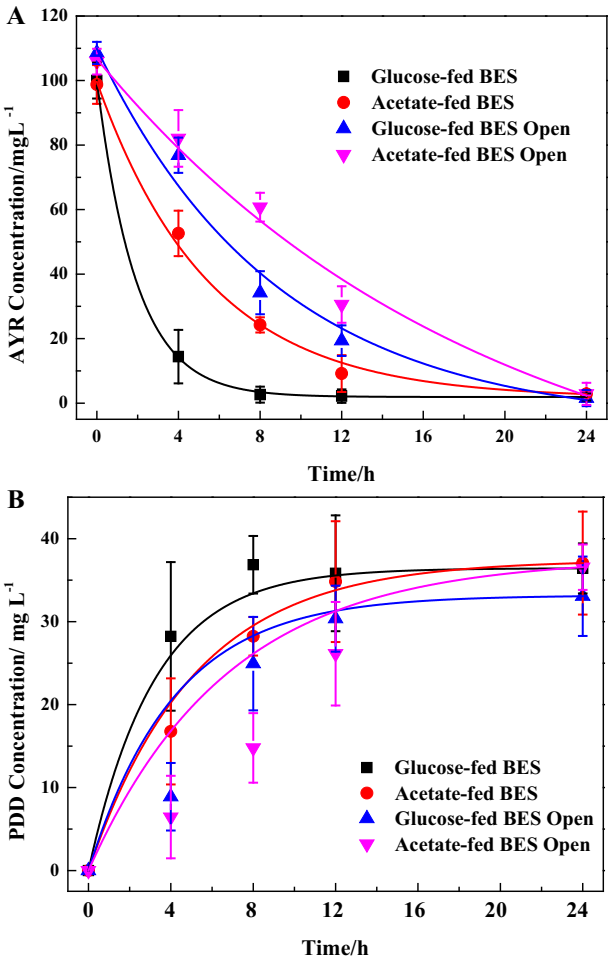


**Fig. 1.** AYR reductive decolorization fed with acetate and glucose as the co-substrate in BESs. (A) Concentration changes of AYR in both open and close circuit BESs; (B) concentration changes of the generated PPD by AYR decolorization in both open and close circuit BESs. In all constructed systems, the applied voltage and the initial AYR concentration were 0.5 V and 100 mg $L^{-1}$, respectively.

### 3.2. Electrochemical properties of glucose/acetate-fed biocathode for AYR decolorization

The electrochemical behavior of biocathode for AYR reductive decolorization was tested with cyclic voltammetry (CV) (Fig. 2A). After applying AYR, two irreversible reductive peaks, one remarkable and another less obvious, were appeared at −0.92 V (vs. SCE, remarkable) and −0.59 V (vs. SCE, less obvious), respectively, whether fed with glucose or acetate. The two peaks corresponded to the two reduction peaks of nitro ($-NO_2^-$) and azo bonds (–N=N–) (Cui et al., 2012). The absolute current of $|I_{acetate}|$ was higher than $|I_{glucose}|$, suggested that the cathodic biofilm was more active fed with acetate than glucose, although the high decolorization efficiency was shown up under glucose-fed conditions.

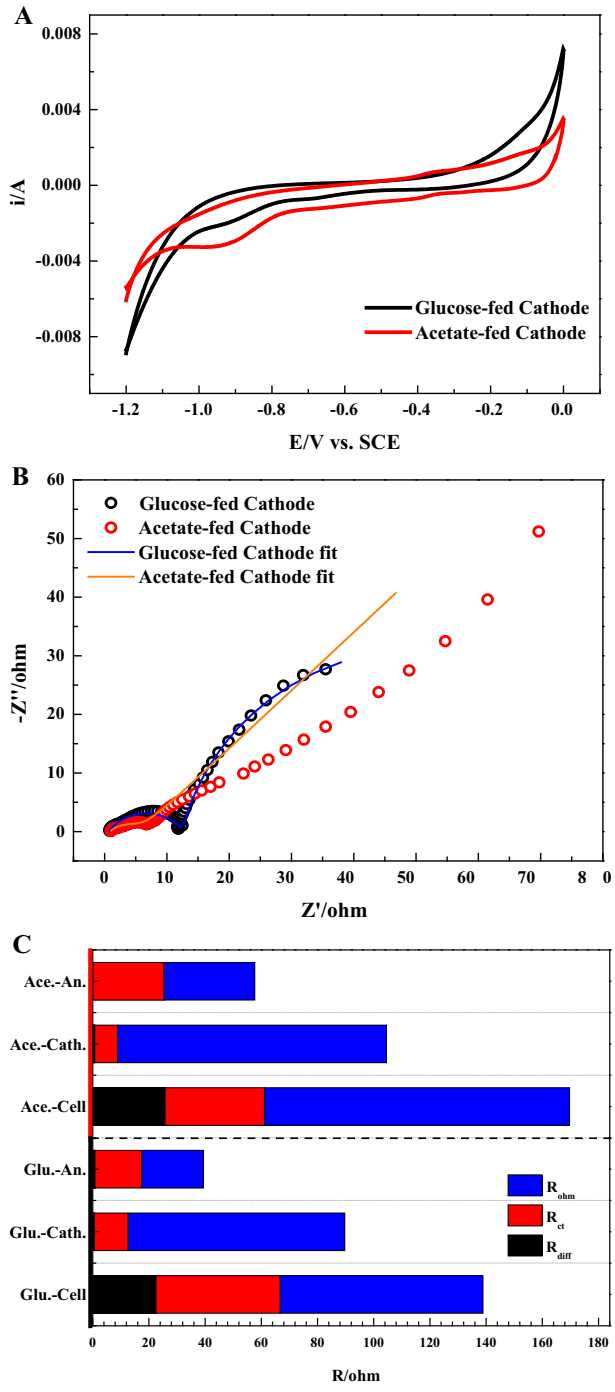


**Fig. 2.** Electrochemical characteristic analysis fed with acetate and glucose as the carbon sources in BESs for AYR decolorization. (A) Cyclic voltammetry (CV, scan rate: 1 mV/s) in closed circuit with AYR of 100 mg $L^{-1}$; (B) Nyquist plots in cathode by EIS; (C) ohmic internal resistance in anode, cathode, and the whole cell calculated by EIS and Nyquist plots. "Ace.-An" indicated the anodic resistance in acetate-fed condition; "Ace.-Cath." indicated the cathodic resistance in acetate-fed condition; "Ace.-Cell." indicated the resistance of the whole cell in acetate-fed condition; "Glu.-An" indicated the anodic resistance in glucose-fed condition; "Glu.-Cath." indicated the cathodic resistance in glucose-fed condition; "Glu.-Cell." indicated the resistance of the whole cell in glucose-fed condition.

Robustness of the electrochemically-active biofilms were a central performance indicator to prospect industrially-relevant BES that use microorganisms as the electrocatalytic entity (Sharma et al., 2014). Impedance response of the whole cell, anode and cathode in dual-chamber BES were analyzed, as shown by Nyquist plots (Fig. 2B) and *R* analysis (Fig. 2C). $R_{ohm}$ of the cell, cathode and anode were 22.5, 0.60 and 0.79 Ω (glucose-fed biocathode), and 25.74, 0.82 and 0.16 Ω (acetate-fed biocathode), respectively. The results showed the apparent drop of the total resistance in BES fed with glucose compared with acetate. As calculated, the total resistance was about 73.2% of lower fed with glucose than acetate, indicated that glucose-fed cathodic biofilm accelerated the electron transfer process. The low resistance and efficient electron transfer process obviously speeded up the AYR decolorization efficiency (Fig. 1).

### 3.3. Richness and diversity of bacterial phylotypes

Three 16S rRNA gene libraries were constructed from MiSeq sequencing of bacteria communities in glucose- and acetate-fed cathodic biofilm and the raw sludge that inoculated to cathode (RAW), with 25,323, 29,463, and 24,212 of high-quality reads (average length of 455 bp), respectively (SI Fig. S1 and Table S2). Totally 1681 (glucose-fed biocathode), 2040 (acetate-fed biocathode) and 4457 (Raw) operational taxonomic unites (OTUs) at a 3% distance were obtained. RAW had the greatest richness than glucose- and acetate-fed biocathode, caused by the directional selection of bacteria on electrode which made the loss of biodiversity. Shannon diversity index provided the species richness, that the raw had the highest diversity (Shannon = 6.82) among the three communities, and acetate-fed biocathode (4.91) was slightly larger than 4.13 in glucose-fed biocathode. The different types of carbon sources caused changes with respect to the relative abundance of bacteria communities and also the dominant bacterial species.

### 3.4. Comparative analysis of bacterial communities

Hierarchical cluster analysis was applied to identify the differences of the three bacterial community structures (Fig. 3A). The glucose-fed and acetate-fed biocathodes were separated from the Raw, suggesting the clear distinctions of community structure, despite that they shared the same source of bacterial consortia. This was supported by the principal component analysis (PCA) (Fig. 3B). Principal components 1 and 2 explained 73.9% and 26.1% of the total community variations, respectively. Two biocathode samples were clustered together, but still, the clear distinction was represented in glucose-fed and acetate-fed ones. Both of them showed the visible difference from Raw. The sum of total observed OTUs in all three communities was 2559, but only 136 OTUs or 5.3% of the total OTUs were shared by them (Fig. 3C). The majority (74.8%) of the shared OTUs were *Proteobacteria* (43.6%), *Firmicutes* (16.4%) and *Bacteroidetes* (14.8%). Glucose- and acetate-fed biocathode had the more common OTUs (239% and 9.3% of total) than any of them with Raw. OTUs that were unique to each community numbered 397 (glucose-fed BES), 471 (acetate-fed BES) and 1047 (Raw), and the together accounted for 74.8% of the total number of observed OTUs.

### 3.5. Bacterial taxonomic identification in phylum and class levels

To identify the phylogenetic diversity of bacterial communities in biocathodes and Raw, the qualified reads to understand phyla, classes and genera were assigned (Fig. 4). Three communities showed the extremely high diversities, reflected that 21 (glucose-fed), 18 (acetate-fed) and 19 (RAW) of identified phyla were observed (Fig. 4A). Among of them, *Proteobacteria*, *Bacteroidetes* and *Firmicutes* were the most abundant. The sum of the three phyla accounted for 91.9% (glucose-fed), 79.4% (acetate-fed) and 57.8% (Raw) of the total reads, respectively. *Proteobacteria* was more abundant in glucose-fed (52.5%) and acetate-fed biocathode

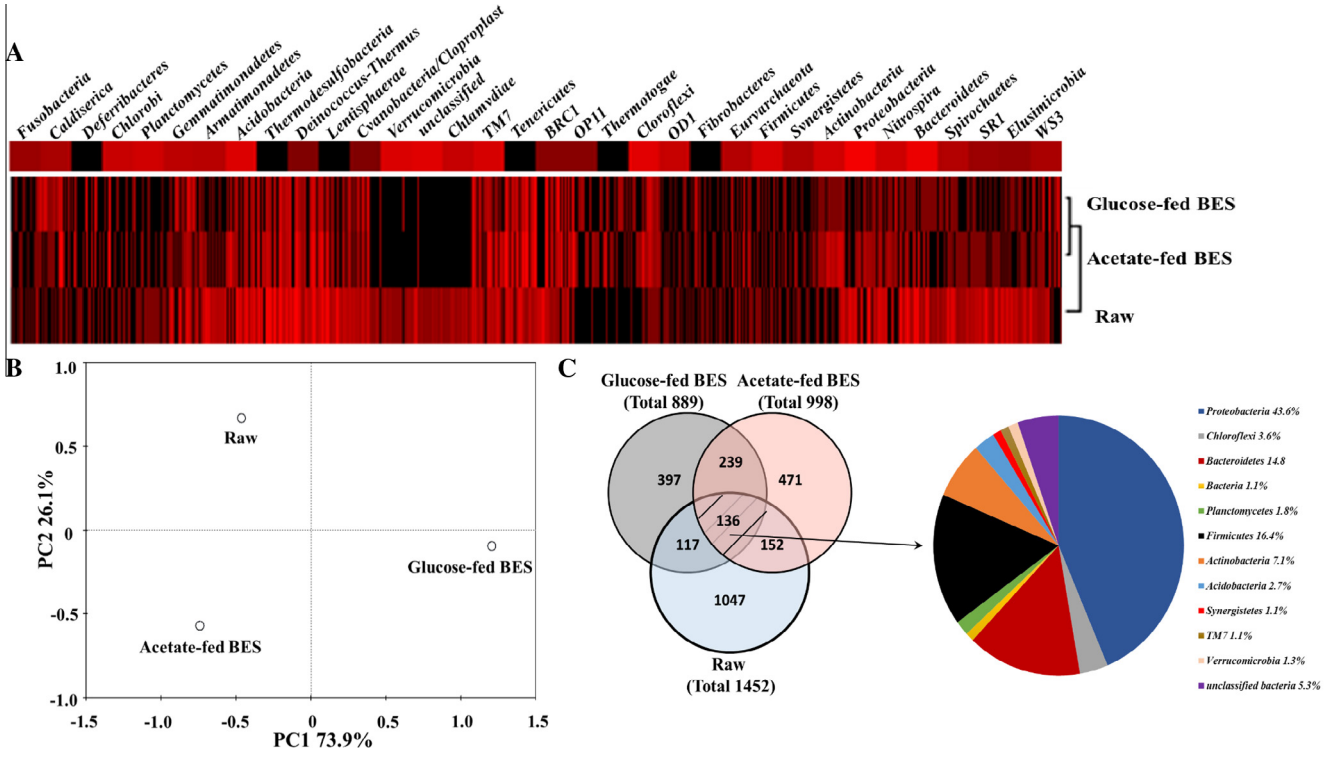


**Fig. 3.** (A) Hierarchical cluster analysis of bacterial communities in glucose-fed cathode, acetate-fed cathode and raw sludge (RAW). The *y*-axis is the clustering of the 300 most abundant OTUs (3% distance) in reads. The OTUs were ordered by phylum. Sample communities were clustered based on complete linkage method, the color intensity of scale indicated relative abundance of each OTU read. Relative abundance was defined as the number of sequences affiliated with that OUT divided by the total number of sequences per sample. (B) Principal component analysis (PCA) of bacterial communities from glucose-fed cathode, acetate-fed cathode and raw sludge (RAW) based on pyrosequencing of 16S rRNA gene. (C) Overlap of the three bacterial communities from samples in glucose-fed cathode, acetate-fed cathode and the raw sludge samples (RAW) based on OUT (over 97% of similarity), and the taxonomic identities of the shared OTUs at phylum level. The number in parentheses represents the total number of OTUs in the community.

(65.8%), compared with Raw (34.9%). *Firmicutes* was the lowest in Raw (4.1%) and the highest in glucose-fed biocathode (21.0%). In comparison, *Bacteroidetes* represented the similar abundance among the three communities. *Actinobacteria* and *Euryarchaeota* are predominated in acetate-fed biocathode than glucose-fed biocathode. *Chloroflexi*, the commonly found filamentous phyla during wastewater treatment processes, was dominated in Raw.

MiSeq sequencing detected 57 bacterial classes in all three communities and the majority of sequences belonged to 10 classes (Fig. 4B). Glucose-fed biocathode and acetate-fed biocathode were quite different from Raw in level of class. *Gammaproteobacteria* (39.5%), *Bacteroidia* (16.1%) and *Bacilli* (15.2%) belonged to phyla of *Proteobacteria* and *Firmicutes* were obviously enriched in glucose-fed biocathode compared to those of the initial inoculum, and all of them showed the decrease trend in acetate-fed biocathode. However, *Beta-proteobacteria* (27.2%) and *Alpha-proteobacteria* (9.7%) were predominant only in acetate-fed biocathode. In comparison, Raw sample was primarily consisted of *Gammaproteobacteria* (11.9%), *Sphingobacteria* (11.1%), *Betaproteobacteria* (8.4%) and *Alphaproteobacteria* (9.1%).

### 3.6. Bacterial taxonomic identification in genus level

Standing on the genus level, a total of 503 genera were classified among these samples and 43 genera with the relative abundance over 1% in the initial inoculum (Raw), glucose-fed biocathode and acetate-fed biocathode were shown in Fig. 4 and SI Table S3. The bacterial community showed the remarkable diverse general composition in both abundance and types. For sample Raw, the genera with abundance less than 1% occupied the largest composition (66.8%), including *Dokdonella*, *Longilinea*, *Luteolibacter*, *Haliscomenobacter* and etc. As statistics, more than 491 types of genera were observed (data not shown), suggesting the wide variety of community structure.

After the directional enrichment in biocathode, the bacterial composition altered. *Citrobacter* (29.2%), *Enterococcus* (14.7%), *Alkaliflexus* (9.2%) and *Paludibacter* (4.5%) had obviously higher relative abundance in glucose-fed biocathode than those in the Raw or acetate-fed biocathode. Among of them, *Citrobacter* sp., which have been previously reported that could decolorize several recalcitrant dyes in presence of glucose, except bromophenol blue (Wang et al., 2009a), occupied the largest bacterial community composition. *Enterococcus* sp., belong to Bacilli, possessed the second largest group of bacterial genera. Purification and characterization of azoreductase enzymes in *Enterococcus faecalis*, suggested the highest specific azoreductase activity (Chen et al., 2004). Also, *Enterococcus* sp. was reported that could generate electricity in MFC without the providing of an exogenous mediator (Cristiani et al., 2013). *Paludibacter*, the fermentative bacteria, was also determined with the relative low abundance.

In acetate-fed biocathode, *Acinetobacter* (17.8%), *Achromobacter* (6.4%), *Comamonas* (2.5%), *Stenotrophomonas* (2.7%) and *Fluviicola* (5.0%) were remarkably enriched, and however, they represented the fewer abundance in Raw and glucose-fed biocathode. As noticed, *Acinetobacter* sp. was one of the dominant active ones, which have been reported that was able to degrade various types of aromatic hydrocarbons, include azo dyes (Ghodake et al., 2009). *Acinetobacter* sp. was also responsible for electroacetogenesis through directly electron transfer from bacteria to electrode (Zhang et al., 2011). *Achromobacter* sp., the azo dye dechlorization bacterial species, like malachite green (Wang et al., 2011), were specially enriched. However, the extracellular electron transfer

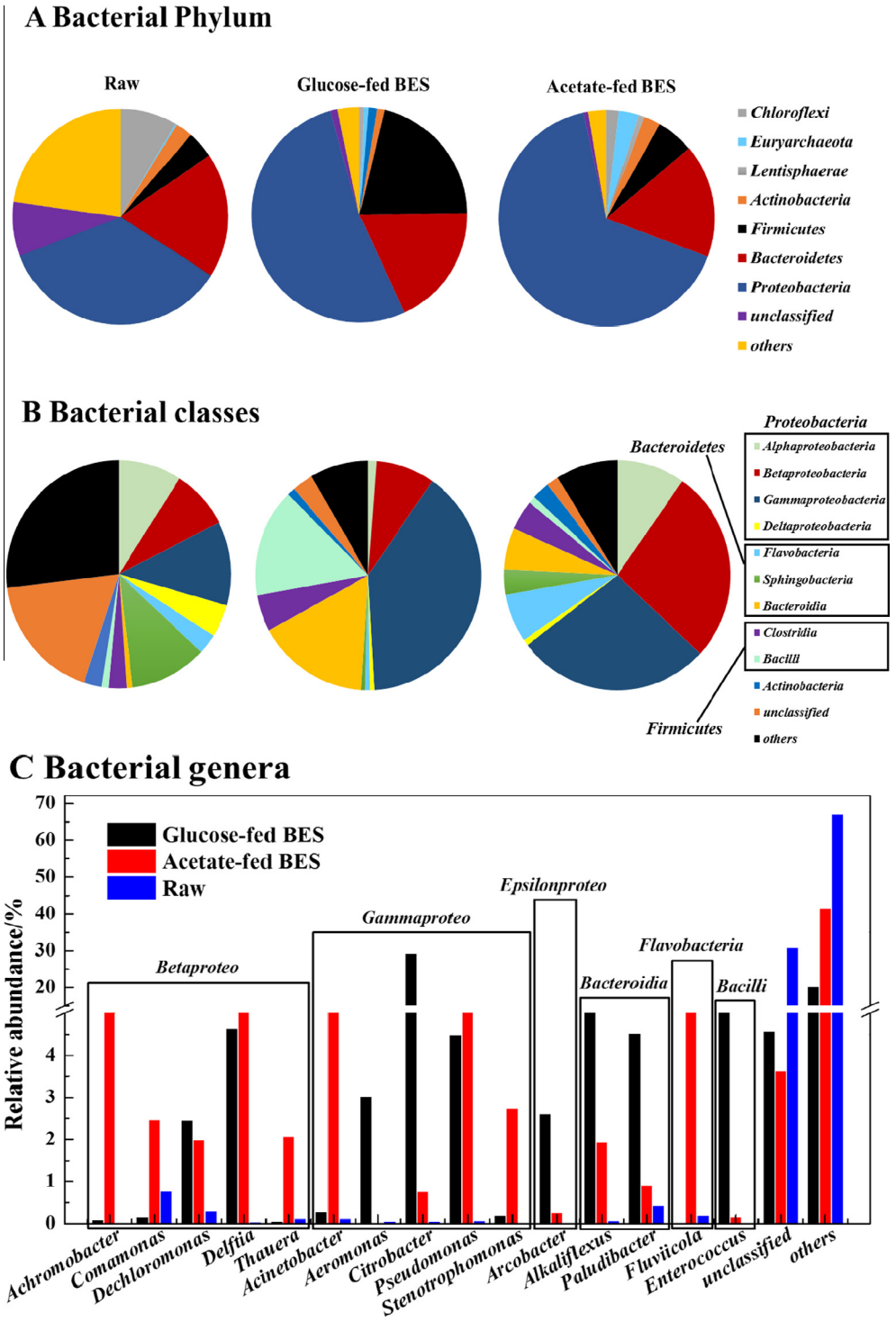


**Fig. 4.** Taxonomic classification of MiSeq sequencing from bacterial communities of raw sludge sample (RAW), glucose-fed biocathode and acetate-fed biocathode at (A) phylum, (B) class and (C) genus levels. Relative abundance was defined as the number of sequences affiliated with that taxon divided by the total number of sequences per sample. Phyla, classes, and genera making up less than 1% of total composition in all three libraries were classified as "others". The detailed classification in level of genus was distributed in Supplementary information Table S3.

capacity of *Achromobacter* sp. has not yet been determined (Zhang et al., 2012). *Comamonas* sp. was reported that could decoloriate the azo dyes, such as the direct blue GLL; meanwhile, the electrode active strain has been isolated from cathodic biofilm (Xing et al., 2010). *Stenotrophomonas* sp. was able to reductive decolorizate Acid Red 88, and was also reported that could be largely enriched in cathodic biofilm (Zhang et al., 2012).

Besides, *Pseudomonas* (7.8% and 4.5% for acetate- and glucose-fed), *Delftia* (9.4% and 4.7% for acetate- and glucose-fed), *Dechloromonas* (2.0% and 2.5% for acetate- and glucose-fed) and *Alkaliflexus* (1.9% and 9.2% for acetate- and glucose-fed) were simultaneous enriched in cathode fedding with either glucose or acetate. *Pseudomonas* sp. has been widely reported that could directly transfer electrons to electrode by oxidation (Raghavulu et al., 2011), or

through generation of electron shuttles to promote electrode–microbe electron transfer (Pham et al., 2008). Also, some pure strains belonging this genus were isolated that could decolorizate various types of azo dye (Hsueh and Chen, 2008). *Dechloromonas* sp. have been reported that was able to reduce nitrate, perchlorate and etc. in biocathode (Coates et al., 2001). *Delftia* sp. has been widely reported that found in BESs holding the reductive decolorization capacity of azo dyes by pure strain (Stolze et al., 2012; Zhang et al., 2013).

### 3.7. Outlook

The results showed the less bacterial community diversity (SI Fig. S1 and Table S2) and clear distinctions of phylotype structure (Fig. 3A and B) after the sustained electrical field stimulation and successive application of azo dye and co-substrates in biocathode. Some representative genera, such as *Citrobacter*, *Enterococcus*, *Acinetobacter*, *Achromobacter*, *Pseudomonas* and *Delftia*, associated with reductive decolorization, fermentation or directly/indirectly electron transfer with electrode, were selectively enriched (Fig. 4). Previously, Liang et al. (2014) reported the directional reduction of nitrobenzene in biocathode, where *Enterococcus* was selectively enriched as the dominant member. While, some electroactive genera were discovered that facilitated electron transfer by excreting redox mediators in cathodic biofilm. Zhang et al. (2014) reported the conspicuous growth of *Dehalobacter* and *Desulfovibrio* in humin-immobilized cathodic biofilm, which were regarded as that highly associated with pentachlorophenol (PCP) reductive dechlorination. Huang et al. (2012) discovered some genera, such as *Desulfobacterium* and *Fusibacter*, were dominated in biocathode after long-term enrichment for anaerobic mineralization of PCP. The further study for detoxification of heavy metals found the less diversity and the adaptive evolvement of bacterial community after selective exposure to the mixed metal solutions. These studies supported the selective enrichment of functional species in biocathode, as manistified in this study.

Phylogenetic analysis showed the varied bacterial diversity and structure between glucose-fed and acetate-fed cathodic biofilm, although some representative genera, such as *Pseudomonas*, *Delftia* and etc, were commonly enriched (Fig. 4C and Table S3). This indicated the attached bacterial community was determined by the mode of cathode supplying electrons in respect with the different carbon sources. This is supported by Liang et al. (2014), in which the obvious community structure change was observed with the dominant bacteria varied from heterotrophic *Enterococcus* to autotrophic *Paracoccus* and *Variovorax*, during reduction of nitrobenzene in biocathode. In some MFC reactors, the varied bacterial community was also discovered after supplying with the different co-substrates types. Wang et al. (2012) reported *Gammaproteobacteria* was dominated in acetate-fed MFC and whereas *Firmicutes* was dominated in glucose-fed MFC during PCP degradation. Xing et al. (2009) found the change of co-substrate types impacted both the community structure and electrogenesis efficiency in MFC. Further study would be expected on the morphology and distribution of these functional bacteria.

The varied bacterial community diversity and structure resulted in the distinct decolorization activity and efficiency in glucose/acetate-fed biocathode. The superior capacity was observed with $k$ values (both the decolorization efficiency and metabolite generation efficiency) about twice fed with glucose compared with that fed with acetate (Fig. 1). The results were further supported by electrochemical behavior analysis, where the lower total resistance in glucose-fed BES was observed (Fig. 2). It is indicated that glucose as more efficient as electron donor in faster conversion rate to produce more electrons. The result was consistent with the pervious report by Sun et al. (2009) during reductive decolorization of active brilliant red X-3B. After applying various types of co-subtracts, the maximum decolorization rate was observed with glucose, followed by sucrose, diluted confectionery wastewater and then acetate. Cao et al. (2010) reported the maximum decolorization rate was obtained with glucose, followed by ethanol and acetate, during reductive decolorization of Congo red in air-cathode single-chamber MFC. Wang et al. (2012) found the addition of glucose as co-substrate obviously accelerated the acclimation time and increased the endurance to heavy PCP shock loads than acetate as co-subtract during PCP reduction.

Diverse known electroactive bacterial genera were detected in glucose- and acetate-fed biocathodes, but they were hardly found in Raw, as shown in Table 1. Some of them held the relative high concentration, such as *Pseudomonas*, *Citrobacter* and *Comamonas*. As demonstrated above, *Pseudomonas* sp. could transfer electrons to the electrode via self-produce highly redox-active endogenous electron shuttles such as pyocyanin. Wang et al. (2014) applied electrode as sole electrons donor for enhancing decolorization of azo dye with an isolated *Pseudomonas* sp. WYZ-2. It was discovered the electrons were released from electrode, absorbed directly by WYZ-2 and then further arrived at the electron accepter, which efficiently accelerated the electron transfer process. Xu and Liu (2011) studied the electricity generation capacity with the new *Citrobacter* sp. SX-1 supplying with the various carbon sources, and demonstrated that *Citrobacter* sp. transferred electrons to extracellular electron acceptors directly in MFC. *Comamonas denitrificans* was also reported with the exoelectrogenic activity (Xing et al., 2010). Apart from these, others only accounted for small fractions in bacterial community. *Shewanella* sp. could utilize the outer membrane cytochromes to transfer electrons with electrode directly, or indirectly by extruding the electrically conductive nanowires. *Desulfovibrio desulfuricans* was capable of utilizing natural sulfate/sulfide mediator to generate electricity from lactate in MFC. *Geobacter* sp. could be competent to produce conductive pili that account for direct electron transfer. Also, both *Shewanella* sp. and *Geobacter* sp. has been reported that could utilize electron as the sole electron donor for reductive dechlorination of various types of chloroethanes (Cretnik et al., 2013). Attraction of the various types of electroactive bacteria evinced their direct or indirect

**Table 1**
Relative abundance of the known electroactive genera in bacterial communities of the inoculated raw sludge (Raw), glucose-fed biocathode and acetate-fed biocathode.

| Electroactive genera | % of abundance of the total reads | | |
|---|---|---|---|
| | Raw | Glucose-fed biocathode | Acetate-fed biocathode |
| *Alcaligenes* | –[a] | 0.18 | 2.5 |
| *Aeromonas* | 0.05 | 3.04 | 0.03 |
| *Arcobacter* | 0.01 | 2.62 | 0.25 |
| *Citrobacter* | 0.05 | 29.24 | 0.77 |
| *Clostridium* | 0.02 | 0.04 | 0.09 |
| *Comamonas* | 0.78 | 0.15 | 2.47 |
| *Desulfobulbus* | 0.1 | – | – |
| *Desulfovibrio* | 0.07 | 0.28 | 0.13 |
| *Desulfuromonas* | – | 0.03 | 0.08 |
| *Escherichia* | 0.05 | 0.05 | 0.06 |
| *Geobacter* | 0.09 | 0.09 | 0.52 |
| *Geopsychrobacter* | 0.05 | – | – |
| *Geothrix* | 0.5 | 0.02 | 0.03 |
| *Klebsiella* | – | 0.41 | 0.08 |
| *Lysinibacillus* | 0.01 | 0.26 | 0.5 |
| *Ochrobactrum* | – | 0.06 | 0.67 |
| *Pseudomonas* | 0.07 | 4.49 | 7.76 |
| *Rhodoferax* | 0.08 | – | 0.01 |
| *Shewanella* | – | 0.06 | 0.01 |

[a] "–" indicated undetectable through the high-throughput 16S rRNA gene sequencing analysis.

participation of electron transfer between electrode and contaminant (AYR).

Selective enrichment of cathodic bacterial community was investigated during reductive decolorization of AYR fedding with glucose or acetate as co-substrates in BESs. The bacterial community became less diverse and the clear distinctions of phylotype structures were observed after the sustained electrical field stimulation and application of AYR and co-substrates. Most of the dominant genera found were capable of reducing azo dyes, that, *Citrobacter*, *Enterococcus*, *Alkaliflexus* and etc. were dominant in glucose-fed biocathode, and while, *Acinetobacter*, *Achromobacter* and etc. were predominant in acetate-fed biocathode. The distinct bacterial community resulted in the different treatment efficiency, and the maximum decolorization rate of AYR ($k_{AYR}$ = 0.46 $h^{-1}$) and PPD generation rate ($k_{PPD}$ = 0.38 $h^{-1}$) were obtained fedding with glucose as co-substrate. Besides, diverse known electrode active bacterial genera were discovered in cathodic biofilm. The results revealed that the supplement of the different co-substrate types impacted the performance (decolorization efficiency and rate) and also significantly altered the structure, richness and composition of cathodic bacterial communities during reductive decolorization of azo dyes in BESs.

## 4. Conclusions

Collectively, the study found the selective enrichment of cathodic bacterial communities fed with glucose or acetate as co-substrates during reductive decolorization of AYR in biocathode. Most of the dominant genera were capable of reducing azo dyes, that, Citrobacter, Enterococcus and Alkaliflexus in glucose-fed biocathode, and while, Acinetobacter and Achromobacter in acetate-fed biocathode. Some known electrode active bacterial genera were discovered. The maximum AYR decolorization rate ($k_{AYR}$ = 0.46) and PPD generation rate ($k_{PPD}$ = 0.38) were obtained fedding with glucose. Supplement of the different co-substrate types impacted the performance and altered the structure and composition of bacterial communities during decolorization of azo dyes.

## Acknowledgements

This study was supported by the National Natural Science Foundation of China – China (NSFC, No. 31400104), by National Science Foundation for Distinguished Young Scholars – China (Grant No. 51225802), by the National High-tech R&D Program of China – China (863 Program, Grant No. 2011AA060904), by the Major Science and Technology Program for Water Pollution Control and Treatment – China (No. 2014ZX07204-005), by "Hundred Talents Program" of the Chinese Academy of Sciences, by Project 135 of Chinese Academy of Sciences – China (No. YSW2013B06), and by Science and Technology Service Network Initiative of Chinese Academy of Sciences – China (No. KFJ-EW-STS-102).

## Appendix A. Supplementary data

Supplementary data associated with this article can be found, in the online version, at http://dx.doi.org/10.1016/j.biortech.2016.02.003.

## References

Cao, Y.Q., Hu, Y.Y., Sun, J.A., Hou, B., 2010. Explore various co-substrates for simultaneous electricity generation and Congo red degradation in air-cathode single-chamber microbial fuel cell. Bioelectrochemistry 79 (1), 71–76.

Chen, H.Z., Wang, R.F., Cerniglia, C.E., 2004. Molecular cloning, overexpression, purification, and characterization of an aerobic FMN-dependent azoreductase from *Enterococcus faecalis*. Protein Express. Purif. 34 (2), 302–310.

Coates, J.D., Chakraborty, R., Lack, J.G., O'Connor, S.M., Cole, K.A., Bender, K.S., Achenbach, L.A., 2001. Anaerobic benzene oxidation coupled to nitrate reduction in pure culture by two strains of *Dechloromonas*. Nature 411 (6841), 1039–1043.

Cretnik, S., Thoreson, K.A., Bernstein, A., Ebert, K., Buchner, D., Laskov, C., Haderlein, S., Shouakar-Stash, O., Kliegman, S., McNeill, K., Elsner, M., 2013. Reductive dechlorination of TCE by chemical model systems in comparison to dehalogenating bacteria: insights from dual element isotope analysis (C-13/C-12, Cl-37/Cl-35). Environ. Sci. Technol. 47 (13), 6855–6863.

Cristiani, P., Franzetti, A., Gandolfi, I., Guerrini, E., Bestetti, G., 2013. Bacterial DGGE fingerprints of biofilms on electrodes of membraneless microbial fuel cells. Int. Biodeterior. Biodegrad. 84, 211–219.

Cui, D., Guo, Y.Q., Cheng, H.Y., Liang, B., Kong, F.Y., Lee, H.S., Wang, A.J., 2012. Azo dye removal in a membrane-free up-flow biocatalyzed electrolysis reactor coupled with an aerobic bio-contact oxidation reactor. J. Hazard. Mater. 239, 257–264.

Cui, D., Guo, Y.Q., Lee, H.S., Cheng, H.Y., Liang, B., Kong, F.Y., Wang, Y.Z., Huang, L.P., Xu, M.Y., Wang, A.J., 2014. Efficient azo dye removal in bioelectrochemical system and post-aerobic bioreactor: optimization and characterization. Chem. Eng. J. 243, 355–363.

ElMekawy, A., Srikanth, S., Bajracharya, S., Hegab, H.M., Nigam, P.S., Singh, A., Mohan, S.V., Pant, D., 2015. Food and agricultural wastes as substrates for bioelectrochemical system (BES): the synchronized recovery of sustainable energy and waste treatment. Food Res. Int. 73, 213–225.

Ghodake, G.S., Kalme, S.D., Jadhav, J.P., Govindwar, S.P., 2009. Purification and partial characterization of lignin peroxidase from *Acinetobacter calcoaceticus* NCIM 2890 and its application in decolorization of textile dyes. Appl. Biochem. Biotechnol. 152 (1), 6–14.

Hsueh, C.C., Chen, B.Y., 2008. Exploring effects of chemical structure on azo dye decolorization characteristics by *Pseudomonas luteola*. J. Hazard. Mater. 154 (1–3), 703–710.

Huang, L.P., Chai, X.L., Quan, X., Logan, B.E., Chen, G.H., 2012. Reductive dechlorination and mineralization of pentachlorophenol in biocathode microbial fuel cells. Bioresour. Technol. 111, 167–174.

Huang, L.P., Cheng, S.A., Chen, G.H., 2011. Bioelectrochemical systems for efficient recalcitrant wastes treatment. J. Chem. Technol. Biotechnol. 86 (4), 481–491.

Iyappan, S. et al., 2010. Biodegradation and decolorization of Acid Red by *Acinetobacter radioresistens*. J. Biorem. Biodegrad. 1 (1).

Liang, B., Cheng, H.Y., Van Nostrand, J.D., Ma, J.C., Yu, H., Kong, D.Y., Liu, W.Z., Ren, N. Q., Wu, L.Y., Wang, A.J., Lee, D.J., Zhou, J.Z., 2014. Microbial community structure and function of nitrobenzene reduction biocathode in response to carbon source switchover. Water Res. 54, 137–148.

Pham, T.H., Boon, N., Aelterman, P., Clauwaert, P., De Schamphelaire, L., Vanhaecke, L., De Maeyer, K., Hofte, M., Verstraete, W., Rabaey, K., 2008. Metabolites produced by *Pseudomonas* sp. enable a Gram-positive bacterium to achieve extracellular electron transfer. Appl. Microbiol. Biotechnol. 77 (5), 1119–1129.

Raghavulu, S.V., Sarma, P.N., Mohan, S.V., 2011. Comparative bioelectrochemical analysis of *Pseudomonas aeruginosa* and *Escherichia coli* with anaerobic consortia as anodic biocatalyst for biofuel cell application. J. Appl. Microbiol. 110 (3), 666–674.

Sharma, M., Bajracharya, S., Gildemyn, S., Patil, S.A., Alvarez-Gallego, Y., Pant, D., Rabaey, K., Dominguez-Benetton, X., 2014. A critical revisit of the key parameters used to describe microbial electrochemical systems. Electrochim. Acta 140, 191–208.

Stolze, Y., Eikmeyer, F., Wibberg, D., Brandis, G., Karsten, C., Krahn, I., Schneiker-Bekel, S., Viehover, P., Barsch, A., Keck, M., Top, E.M., Niehaus, K., Schluter, A., 2012. IncP-1 beta plasmids of *Comamonas* sp. and *Delftia* sp. strains isolated from a wastewater treatment plant mediate resistance to and decolorization of the triphenylmethane dye crystal violet. Microbiology 158, 2060–2072.

Sun, J., Hu, Y., Bi, Z., Cao, Y., 2009. Simultaneous decolorization of azo dye and bioelectricity generation using a microfiltration membrane air-cathode single-chamber microbial fuel cell. Bioresour. Technol. 100 (13), 3185–3192.

Sun, J., Li, Y., Hu, Y., Hou, B., Zhang, Y., Li, S., 2013. Understanding the degradation of Congo red and bacterial diversity in an air-cathode microbial fuel cell being evaluated for simultaneous azo dye removal from wastewater and bioelectricity generation. Appl. Microbiol. Biotechnol. 97 (8), 3711–3719.

Sun, Q., Li, Z.L., Wang, Y.Z., Cui, D., Liang, B., Thangavel, S., Chung, J.S., Wang, A.J., 2015. A horizontal plug-flow baffled bioelectrocatalyzed reactor for the reductive decolorization of Alizarin Yellow R. Bioresour. Technol. 195, 73–77.

Tan, N.C., Lettinga, G., Field, J.A., 1999. Reduction of the azo dye Mordant Orange 1 by methanogenic granular sludge exposed to oxygen. Bioresour. Technol. 67 (1), 35–42.

van der Zee, F.P., Villaverde, S., 2005. Combined anaerobic-aerobic treatment of azo dyes – a short review of bioreactor studies. Water Res. 39 (8), 1425–1440.

Wang, H., Su, J.Q., Zheng, X.W., Tian, Y., Xiong, X.J., Zheng, T.L., 2009a. Bacterial decolorization and degradation of the reactive dye Reactive Red 180 by *Citrobacter* sp. CK3. Int. Biodeterior. Biodegrad. 63 (4), 395–399.

Wang, J.A., Qiao, M., Wei, K.B., Ding, J.M., Liu, Z.Z., Zhang, K.Q., Huang, X.W., 2011. Decolorizing activity of malachite green and its mechanisms involved in dye biodegradation by *Achromobacter xylosoxidans* MG1. J. Mol. Microbiol. Biotechnol. 20 (4), 220–227.

Wang, S.S., Huang, L.P., Gan, L.L., Quan, X., Li, N., Chen, G.H., Lu, L., Xing, D.F., Yang, F. L., 2012. Combined effects of enrichment procedure and non-fermentable or fermentable co-substrate on performance and bacterial community for pentachlorophenol degradation in microbial fuel cells. Bioresour. Technol. 120, 120–126.

Wang, Y.Q., Zhang, J.S., Zhou, J.T., Zhang, Z.P., 2009b. Biodegradation of 4-aminobenzenesulfonate by a novel *Pannonibacter* sp. W1 isolated from activated sludge. J. Hazard. Mater. 169 (1–3), 1163–1167.

Wang, Y.Z., Wang, A.J., Zhou, A.J., Liu, W.Z., Huang, L.P., Xu, M.Y., Tao, H.C., 2014. Electrode as sole electrons donor for enhancing decolorization of azo dye by an isolated *Pseudomonas* sp. WYZ-2. Bioresour. Technol. 152, 530–533.

Xing, D.F., Cheng, S.A., Logan, B.E., Regan, J.M., 2010. Isolation of the exoelectrogenic denitrifying bacterium *Comamonas denitrificans* based on dilution to extinction. Appl. Microbiol. Biotechnol. 85 (5), 1575–1587.

Xing, D.F., Cheng, S.A., Regan, J.M., Logan, B.E., 2009. Change in microbial communities in acetate- and glucose-fed microbial fuel cells in the presence of light. Biosens. Bioelectron. 25 (1), 105–111.

Xu, S., Liu, H., 2011. New exoelectrogen *Citrobacter* sp. SX-1 isolated from a microbial fuel cell. J. Appl. Microbiol. 111 (5), 1108–1115.

Zhang, D.D., Zhang, C.F., Li, Z.L., Suzuki, D., Komatsu, D.D., Tsunogai, U., Katayama, A., 2014. Electrochemical stimulation of microbial reductive dechlorination of pentachlorophenol using solid-state redox mediator (humin) immobilization. Bioresour. Technol. 164, 232–240.

Zhang, G.D., Zhao, Q.L., Jiao, Y., Wang, K., Lee, D.J., Ren, N.Q., 2012. Biocathode microbial fuel cell for efficient electricity recovery from dairy manure. Biosens. Bioelectron. 31 (1), 537–543.

Zhang, G.D., Zhao, Q.L., Jiao, Y., Zhang, J.N., Jiang, J.Q., Ren, N., Kim, B.H., 2011. Improved performance of microbial fuel cell using combination biocathode of graphite fiber brush and graphite granules. J. Power Sources 196 (15), 6036–6041.

Zhang, G.Y., Zhang, H.M., Zhang, C.Y., Zhang, G.Q., Yang, F.L., Yuan, G.G., Gao, F., 2013. Simultaneous nitrogen and carbon removal in a single chamber microbial fuel cell with a rotating biocathode. Process Biochem. 48 (5–6), 893–900.